NUMERICAL DISPERSION IN THE FINITE-ELEMENT METHOD USING THREE-DIMENSIONAL EDGE ELEMENTS

Gregory S. Warren[1] **and Waymond R. Scott, Jr.**[1]
[1] School of Electrical and Computer Engineering
Georgia Institute of Technology
Atlanta, Georgia 30332-0250

Received 28 January 1998

ABSTRACT: *The discretization inherent in the vector finite-element method results in the numerical dispersion of a propagating wave. The numerical dispersion of a time-harmonic plane wave propagating through an infinite, three-dimensional, finite-element mesh composed of hexahedral and tetrahedral edge elements is investigated in this work. The effects on the numerical dispersion of the propagation direction of the wave and the electrical size of the elements are investigated. The numerical dispersion of the tetrahedral edge elements is found to be dependent upon the polarization of the plane wave propagating through the mesh. In addition, the dispersion of the tetrahedral elements is significantly smaller than the dispersion of the hexahedral edge elements. Both elements are found to have a phase error that converges at the rate of* $O[(h/\lambda)^2]$.
 Microwave Opt Technol Lett 18: 423–429, 1998.

Key words: *finite-element method; numerical dispersion; wave propagation*

I. INTRODUCTION

The finite-element method is a popular technique in computational electromagnetics for solving three-dimensional vector field problems. For this type of application, "edge" elements are commonly used to discretize the domain of interest [1–4]. In an edge element, the unknowns of the field approximation are associated with the magnitude and direction of the field along the edges of the element. These elements are useful because they do not give rise to spurious solutions as do the more traditional nodal elements [5]. In addition, boundary conditions are generally easier to impose when edge elements are used rather than nodal elements.

In a finite element, whether it be edge or nodal, a significant error arises from the inability of the polynomial basis functions to represent the field exactly. A wave propagating through a finite-element mesh will experience numerical dispersion as a result of this error. The numerical dispersion of one-dimensional and two-dimensional, nodal and edge element meshes has been investigated [6–10]. The results from these investigations are useful when applying the finite-element method in determining the necessary electrical size of the elements to ensure a certain maximum dispersion. The real utility of the edge element is in its application to three-dimensional problems; however, the numerical dispersion associated with three-dimensional edge elements has not been quantified. As a result, the numerical dispersion of the most common three-dimensional edge elements is investigated in this work. Results are presented which are useful for determining the necessary electrical size of the edge elements when applying the finite-element method to three-dimensional problems.

Two types of edge elements are commonly used: the hexahedral element and the tetrahedral element. The numerical dispersion of a time-harmonic plane wave propagating through an infinite, three-dimensional, finite-element mesh composed of hexahedral and tetrahedral edge elements is determined in this work. This numerical dispersion can be characterized by a cumulative phase error. The phase error is quantified as a function of the electrical size of the elements, the direction of propagation of the plane wave through the mesh, and the polarization of the plane wave. It is shown that the phase error for the hexahedral element is simple, and directly reduces to the phase error for the two-dimensional quadrilateral element if the plane wave is restricted to propagate in one of the meshes' principal planes. On the other hand, it is also shown that the phase error for the tetrahedral element is more complicated. In fact, a plane wave with an arbitrary polarization will have its polarization altered as it propagates through the tetrahedral mesh. However, certain linearly polarized plane waves can propagate through the tetrahedral mesh without having their polarizations affected. The phase error of the tetrahedral element mesh is seen to be significantly less than that of the hexahedral mesh. In addition, the phase error for both of the meshes is shown to converge at the rate of $O[(h/\lambda)^2]$.

II. FINITE-ELEMENT METHOD

Consider an infinite, linear, three-dimensional, homogeneous, isotropic, and source-free region. The field in this region is governed by the vector Helmholtz equation:

$$\nabla \times (\nabla \times \mathbf{E}) - k^2 \mathbf{E} = 0 \tag{1}$$

where an $e^{j\omega t}$ time dependence is assumed and $k = \omega\sqrt{\mu\epsilon}$ is the wavenumber. In a finite volume bounded by a surface S such that $S = S_1 + S_2$, the following boundary conditions are used for the finite-element formulation [11]:

$$\hat{n} \times \mathbf{E} = 0 \tag{2}$$

on the portion of the boundary that lies on a perfect electric conductor S_1, and

$$\hat{n} \times (\nabla \times \mathbf{E}) + \gamma\hat{n} \times (\hat{n} \times \mathbf{E}) = \mathbf{U} \tag{3}$$

which is used on all remaining portions of the boundary S_2. The role of this boundary condition is determined by the values of γ and $\mathbf{U}$. In the finite-element method, the volume of interest is subdivided into discrete elements. Then, the vector field is approximated within an element by an expansion in terms of vector basis functions:

$$\tilde{\mathbf{E}}^e = \sum_{i=1}^{n} E_i^e \mathbf{N}_i^e \tag{4}$$

where $\mathbf{N}_i^e$ are the vector basis functions, E_i^e are the unknown coefficients, and n is the number of unknown coefficients. A system of linear equations is obtained by Galerkin's method. The weighted residual for the eth element is [11]

$$R_j^e = \int_{V_e} \mathbf{N}_j^e \cdot [\nabla \times (\nabla \times \tilde{\mathbf{E}}^e) - k^2 \tilde{\mathbf{E}}^e]\, dV, \qquad j = 1, 2, 3, \ldots, n \tag{5}$$

where V^e is the volume enclosed by the element e. Substituting the field expansion into the residual equation and placing it in the "weak form" gives the residual equation for the eth element:

$$\begin{aligned} R_j^e = \sum_{i=1}^{n} E_i^e \Bigg[&\int_{V^e} (\nabla \times \mathbf{N}_j^e) \cdot (\nabla \times \mathbf{N}_i^e)\, dV \\ &- k^2 \int_{V^e} (\mathbf{N}_j^e \cdot \mathbf{N}_i^e)\, dV \\ &+ \gamma \int_{S_2} (\hat{n} \times \mathbf{N}_j^e) \cdot (\hat{n} \times \mathbf{N}_i^e)\, dS \Bigg] \\ &+ \int_{S_2} \mathbf{N}_j^e \cdot \mathbf{U}\, dS, \qquad j = 1, 2, 3, \ldots, n. \end{aligned} \tag{6}$$

The global equations are obtained by expanding the above equation, and then assembling the local equations for all of the elements. The resulting equations are set equal to zero, and the system of linear equations is solved to obtain the unknown coefficients E_i^e. A more detailed explanation is given in [11].

A. Hexahedral Elements. The simplest three-dimensional edge element is the hexahedral or brick element. The element is depicted in Figure 1. In this element, there are 12 edges. Each edge has associated with it an unknown and a vector basis function. The unknowns are the value of the component of the vector field tangent to the edges. The vector basis functions $\mathbf{N}_i^e$ are given in [11]. The basis functions are constructed in such a manner as to ensure continuity of the tangential portion of the vector field across the edges and faces of the element when the elements are assembled to form a mesh.

The first mesh considered is an infinite mesh of hexahedral elements in which the length of all of the edges is h. In this mesh, it is possible to group the edges, and correspondingly the unknowns, according to their relative orientation. It

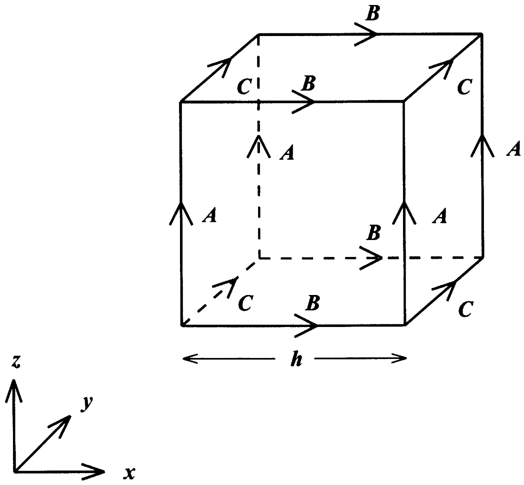

Figure 1 Schematic representation of a first-order, hexahedral edge element. The edges are labeled as belonging to one of three groups: A, B, or C

is easy to see that, for this mesh, there are three groups of edges: the x-directed edges, the y-directed edges, and the z-directed edges. These edges are labeled as A, B, and C, respectively, in Figure 1. The significance of the groups will be discussed in the next section.

B. Tetrahedral Elements. The tetrahedral element is depicted in Figure 2. It is more useful than the hexahedral element because it can model a greater range of geometries. As can be seen, the tetrahedral element has six edges and, correspondingly, six unknowns and six basis functions. As before, the unknowns are the value of the vector field tangent to the edge. The basis functions for the tetrahedral elements are more difficult to construct. A thorough explanation of their construction is provided in [11].

The second mesh considered is an infinite mesh of tetrahedral elements. It is not possible to divide a three-dimensional region into uniform tetrahedral elements. Thus, it is necessary to use a number of different tetrahedral elements to create a three-dimensional mesh. To make the dispersion analysis practical, the mesh must be infinite and periodic. Thus, it is necessary to choose an arrangement of tetrahedral elements that can be assembled to form such a mesh. There are a number of arrangements that can be used, but perhaps the simplest is obtained by dividing a cubical region into five

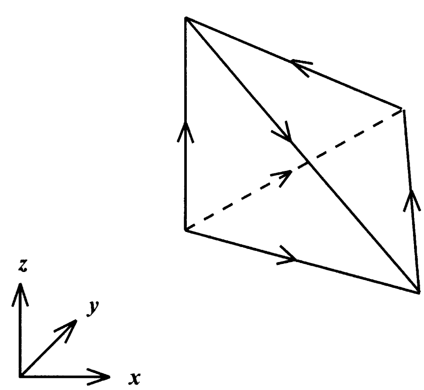

Figure 2 Schematic representation of a first-order, tetrahedral edge element

tetrahedral elements [12]. Consider a uniform cubical region in which each cube has a length, height, and width of h. It is divided up into five elements as in [12]. The volume of four of the elements is $1/6$ that of the cube, and the volume of the fifth element is $1/3$ that of the cube. Through this process, a cubical subcell of tetrahedral elements is obtained which can be assembled into an infinite, periodic, three-dimensional mesh of tetrahedral elements. When the infinite mesh is created, care must be exercised in making sure that the edges of the tetrahedral elements in the cubical subcell align properly. This is accomplished by rotating by 90° every other cubical subcell upon mesh assembly.

For the infinite, quasiuniform mesh created above, it is possible to group the edges in the mesh according to their relative position. This results in 12 separate groups. The significance of the groups will be discussed in the next section.

III. DISPERSION ANALYSIS

Consider a plane wave propagating through an infinite, uniform, and isotropic region with a direction defined by ϕ and θ. It is well known that such a plane wave is an exact solution to the vector Helmholtz equation (1). For this solution, it is easy to show that the field at any point p is related to the field at any other point q by a simple phase factor:

$$\mathbf{E}_q = \mathbf{E}_p e^{-jk\hat{k}\cdot\Delta\mathbf{r}} \tag{7}$$

where $\hat{k} = \sin\theta\cos\phi\hat{a}_x + \sin\theta\sin\phi\hat{a}_y + \cos\theta a_z$ and where $\Delta\mathbf{r}$ is the vector from point p to point q. The relationship in (7) is valid for any polarization of the plane wave.

Now, consider dividing the volume into an infinite, periodic mesh. The field in the mesh will be governed by a discretized vector Helmholtz equation. A plane wave propagating through the mesh at the angles ϕ and θ will also be a solution to the discretized vector Helmholtz equation. However, the plane will propagating with a numerical wavenumber $\tilde{k}$ that differs from the analytical wavenumber k due to the discretization error. In addition, the polarization of the plane wave will not necessarily be preserved as the wave propagates through the mesh. In the special case where p is a point within an element and q is another point at the same relative position within another identical element, the field relationship is still a simple phase factor:

$$\tilde{\mathbf{E}}_q = \tilde{\mathbf{E}}_p e^{-j\tilde{k}\hat{k}\cdot\Delta\mathbf{r}}. \tag{8}$$

Of course, this relationship only holds if the polarization of the plane wave remains constant as it propagates through the mesh.

The purpose of the dispersion analysis is to determine the relationship between the numerical wavenumber $\tilde{k}$ and the analytical wavenumber k, and to determine the polarizations of the plane wave that can propagate through the mesh unaltered. This is accomplished by using the total residual equations for the unknowns in conjunction with the relationship in (8).

In an infinite, uniform mesh, Eq. (6) simplifies to become

$$R_j^e = \sum_{i=1}^{n} E_i^e \left[\int_{V^e} (\nabla \times \mathbf{N}_j^e) \cdot (\nabla \times \mathbf{N}_i^e)\, dV - k^2 \int_{V^e} (\mathbf{N}_j^e \cdot \mathbf{N}_i^e)\, dV \right]. \tag{9}$$

This equation represents the contribution from element e to the residual equation for the unknown j. Consequently, the total residual equation for unknown j is given by

$$R_j = \sum_{e=1}^{m} R_j^e \tag{10}$$

where the index e runs over the m elements which contain the edge with which j is associated.

In an infinite, periodic mesh, it is possible to divide the unknowns into groups whereby the behavior of all of the unknowns within a particular group can be represented by a single total residual equation [10]. Therefore, it is only necessary to consider as many total residual equations as there are groups of unknowns to fully characterize the behavior of the mesh. Thus, since there are three groups of unknowns in the hexahedral mesh, three total residual equations are considered for that mesh, and since there are 12 groups of unknowns in the tetrahedral mesh, 12 total residual equations are considered for that mesh.

A set of nonlinear equations is obtained by substituting (8) into the set of total residual equations. This relationship makes it possible to replace all of the unknowns within a particular group with one unknown from that particular group times a phase factor. This simplification is performed for each group of unknowns, resulting in an equal number of nonlinear equations and unknowns. These equations are very long, and due to space limitations, are not included in this paper.

The construction of the dispersion analysis equations is straightforward to do by hand for a simple two-dimensional mesh [10], but very tedious for three-dimensional meshes. Thus, the process has been implemented numerically. As the values of ϕ and θ are incremented, the computer program iteratively searches for the values of $\tilde{k}$ and plane wave polarization that solve the dispersion relations.

IV. RESULTS

The phase error that results from the dispersion, expressed in degrees per wavelength, is defined as

$$\delta_p = 360\left|\frac{\tilde{k} - k}{k}\right|. \tag{11}$$

A. Hexahedral Mesh. Figure 3 is a graph of the phase error for the hexahedral mesh as a function of propagation direction angles θ and ϕ for $\lambda/h = 20$. In this graph, the phase error is represented by the magnitude of the radial component. For any particular propagation direction, the phase error is the same for any polarization of the plane wave. Thus, a plane wave with any polarization can propagate through the mesh without having its polarization altered. As expected, the error in the x-, y-, and z-planes is exactly the same as the error for the quadrilateral elements. This is because the basis functions for the hexahedral element directly reduce to the basis functions for the quadrilateral element in two dimensions. As can be seen, the phase error is a function of the propagation direction. The maximum phase error is 1.464°/wavelength, and it occurs when the plane wave propagates along one of the coordinate axes. The minimum phase error is 0.492°/wavelength, and it occurs for the propagation angles $\phi_m = 45° + (m-1)90°$ where $m = 1, 2, 3, 4$ and $\theta_m = 90° \pm 35.26°$. An approximation of the numerical wavenumber for $\lambda/h > 5$ is given by

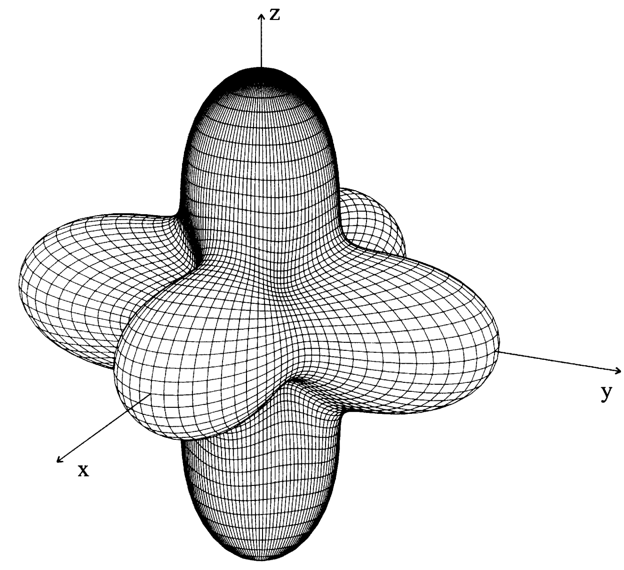

Figure 3 Graph of the phase error in degrees per wavelength of a plane wave propagating through a hexahedral mesh as a function of propagation angles θ and ϕ for $\lambda/h = 20$. The phase error is denoted by the magnitude of the radial component. The maximum phase error is 1.464°/wavelength, and the minimum phase error is 0.492°/wavelength

$$\tilde{k}(\theta, \phi, kh) \approx k + f(\theta, \phi)[\tilde{k}_{1D}(kh) - k] \tag{12}$$

where

$$f(\theta, \phi) = 1 - 2(\cos^2\theta \sin^2\theta + \sin^4\theta \sin^2\phi \cos^2\phi)$$

and

$$\tilde{k}_{1D}(kh) = \frac{1}{h}\cos^{-1}\left[\frac{1 - (kh)^2/3}{1 + (kh)^2/6}\right].$$

$\tilde{k}_{1D}(kh)$ is the numerical wavenumber for a plane wave propagating along one of the coordinate axes of the hexahedral mesh, and it is equivalent to the numerical wavenumber for a plane wave propagating along a one-dimensional, linear, nodal mesh [6].

B. Tetrahedral Mesh. Since the tetrahedral mesh lacks the symmetry of the rectangular mesh and the tetrahedral elements are more complex than the hexahedral element, the phase error of the tetrahedral mesh is much more complicated. In the hexahedral mesh, a plane wave with any polarization could propagate without its polarization changing. However, in the tetrahedral mesh, this can only happen in a few special directions. Thus, for most propagation directions, a generally polarized plane wave will have its polarization changed as it propagates through the tetrahedral mesh. However, for every propagation direction, there are at least two linearly independent polarizations of the plane wave that will be preserved upon propagation through the mesh. These polarizations are linear in nature, and are separated by 90°. Each one of the polarizations has an associated phase error. In a few special directions, the phase error for the two polarizations of the plane wave is the same, and thus, all polarizations will be preserved.

The polarization angle of the plane wave Ψ is depicted in Figure 4. The plane wave has a unit wavevector $\hat{k}$ that is in the direction of the unit radial vector $\hat{e}_r$, defined by the direction angles θ and ϕ. The field **E** essentially lies in the plane orthogonal to the direction of propagation. The orthogonal plane is spanned by the $\hat{e}_\phi$ and $\hat{e}_\theta$ unit vectors defined by the direction angles. The polarization angle Ψ is defined as the angle between **E** and $\hat{e}_\phi$ in this orthogonal plane.

Figure 5 is one of the preserved polarizations for the tetrahedral mesh as a function of propagation direction; the other one of the preserved polarizations is orthogonal to the one shown in Figure 5. In the polarization graph, the **E** vector has been drawn on the surface of a sphere to represent the variation in preserved polarization angle Ψ with propagation direction. In each of the polarization graphs, there are 14 special directions in which a plane wave with any polarization can propagate without having its polarization altered. The six directions that are denoted by the black dots on the sphere in each graph correspond to the coordinate axes directions, and are symmetry directions. The remaining eight directions are denoted by diamonds, and are different in nature. These points are branch points where the continuity of the variation in preserved polarization angle breaks down. The dark lines joining the branch points are branch cuts.

The polarization graph has a complementary graph where the polarization angle is incremented by 180°; $\Psi_{comp} = \Psi + 180°$. The complementary polarization graph can be visualized by simply drawing all of the vectors on the sphere in Figure 5 in the opposite direction. The polarization graph and its complementary graph are "connected" by the branch cuts. In other words, as the propagation direction is varied across the branch cut, it is necessary to leave the polarization graph and jump to its complementary graph to maintain continuity of the polarization angle variation.

Figures 6 and 7 are graphs of the phase error for the tetrahedral mesh as a function of the propagation direction as defined by θ and ϕ for $\lambda/h = 20$. In both figures, the phase error is denoted by the magnitude of the radial component. The phase error for a particular propagation direction is the same for polarizations separated by 180°. Figure 6 is the phase error associated with the preserved polarization angles in Figure 5, and Figure 7 is the phase error associated with the preserved polarization angles that are orthogonal to those in Figure 5. As can be seen, the 14 special points on the spheres in Figure 5 correspond to directions where the phase error for the four sets of polarizations is the same. Thus, any polarization plane wave can propagate in these directions. The maximum phase error for each of the lobes in Figure 6 is 0.187°/wavelength. The maximum phase error in Figure 7 is

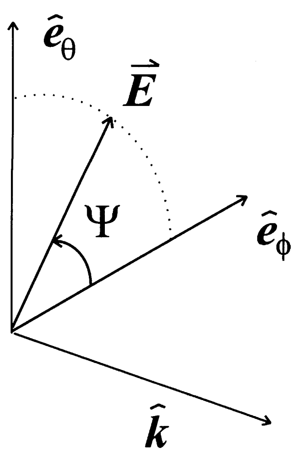

Figure 4 Diagram defining the polarization angle Ψ of a linearly polarized plane wave propagating in the $\hat{k}$-direction. (Note: character with overarrow appears boldface in text.)

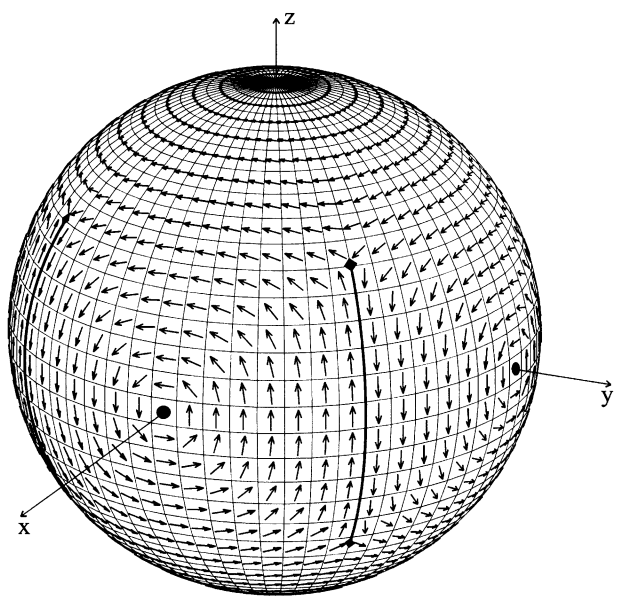

Figure 5 Graph of one set of preserved linear polarizations as a function of θ and ϕ for a plane wave propagating through a mesh of tetrahedral elements. The diamonds denote branch points in the phase angle variation, and the dark lines are branch cuts. The black dots denote symmetry directions

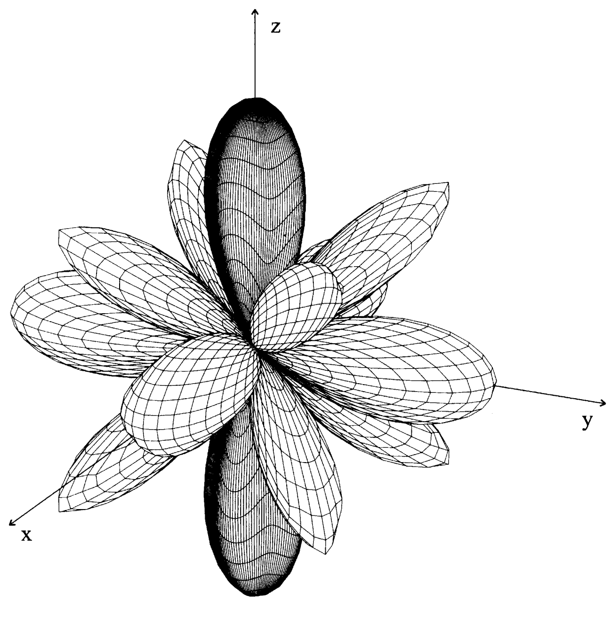

Figure 6 Graph of the phase error in degrees per wavelength of a plane wave having a polarization angle as depicted in Figure 5, and propagating through a tetrahedral mesh with $\lambda/h = 20$. The phase error is denoted by the magnitude of the radial component, and is a function of propagation angles θ and ϕ. The maximum phase error is 0.187°/wavelength

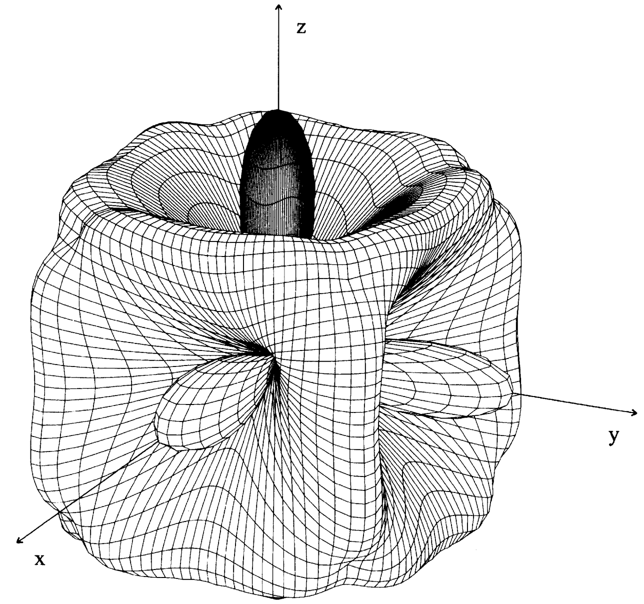

Figure 7 Graph of the phase error in degrees per wavelength of a plane wave having a polarization angle orthogonal to those depicted in Figure 5, and propagating through a tetrahedral mesh with $\lambda/h = 20$. The phase error is denoted by the magnitude of the radial component, and is a function of propagation angles θ and ϕ. The maximum phase error is 0.198°/wavelength

0.198°/wavelength for a plane wave propagating along the directions $\phi_m = (45° \pm 12°) + (m - 1)90°$ and $\theta_m = 90° \pm 40°$ where $m = 1, 2, 3, 4$ and $\phi_m = 45° + (m - 4)90°$ and $\theta_m = 90° \pm 24°$ where $m = 5, 6, 7, 8$. In both figures, there are multiple propagation directions for which the phase error is zero.

The numerical wavenumber $\tilde{k}$ is greater than the analytical wavenumber k for the lobes in Figures 6 and 7 that point along the coordinate axes, and is less than k for the other lobes. For $\lambda/h > 5$, an approximation for the maximum value of $\tilde{k}$ in either Figures 6 and 7 is

$$\tilde{k} \approx k[1 + 0.2073(h/\lambda)^2] \tag{13}$$

and for the minimum value of $\tilde{k}$ is

$$\tilde{k} \approx k[1 - 0.2200(h/\lambda)^2]. \tag{14}$$

The results presented in this study can be used to determine the behavior of an arbitrarily polarized plane wave as it propagates through the tetrahedral mesh. This can be accomplished by decomposing the plane wave into components that lie along the two preserved polarizations for the desired propagation direction. Since each component will propagate with a different wavenumber, the polarization of the plane wave will change as it propagates through the mesh.

C. Rate of Convergence. Figure 8 is a graph of the phase error as a function of the element electrical size λ/h for a plane wave propagating along the x-axis in the tetrahedral and hexahedral meshes. As can be seen, the phase error converges at the rate $O[(h/\lambda)^2]$, which implies that the numerical wavenumber $\tilde{k}$ converges at this rate also. This is the same rate as seen for the two-dimensional quadrilateral mesh [10]. The phase error for the tetrahedral mesh is seen

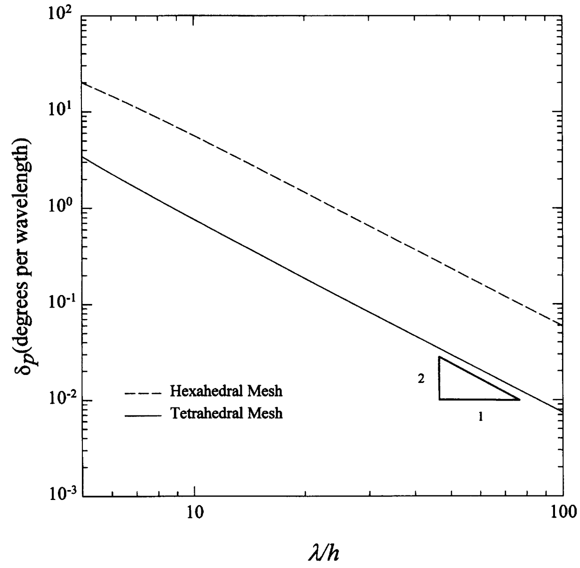

Figure 8 Log–log graph of the phase error in degrees per wavelength for a plane wave propagating in the direction ($\theta = 90°$, $\phi = 0.0°$) through a mesh of hexahedral and tetrahedral edge elements.

to be significantly smaller than the phase error for the hexahedral mesh; however, the tetrahedral mesh has significantly more unknowns than does the hexahedral mesh. This supports the results reported by Chaterjee, Jin, and Volakis that they achieved better accuracy with tetrahedral elements than with hexahedral elements [13].

V. CONCLUSION

The phase error that results from the discretization error in the finite-element method when three-dimensional edge elements are used has been quantified. The error is a function of the propagation direction and the electrical size of the element.

The phase error for the hexahedral elements is straightforward. However, the phase error for the tetrahedral elements is seen to be dependent upon the polarization of the plane wave propagating through the mesh. In fact, for most polarizations, the plane-wave polarization will change as it propagates through the mesh. Finally, the numerical wavenumber $\tilde{k}$ for both of these meshes is seen to converge at the rate of $O[(h/\lambda)^2]$.

REFERENCES

1. A. Bossavit and J. C. Verite, "A Mixed FEM-BIEM Method to Solve 3D Eddy Current Problems," *IEEE Trans. Magn.*, Vol. MAG-18, Mar. 1982, pp. 431–435.
2. M. Hano, "Finite-Element Analysis of Dielectric-Loaded Waveguides," *IEEE Trans. Microwave Theory Tech.*, Vol. MTT-32, Oct. 1984, pp. 1275–1279.
3. M. L. Barton and Z. J. Cendes, "New Vector Finite-Elements for Three-Dimensional Magnetic Field Computation," *J. Appl. Phys.*, Vol. 61, Apr. 1987, pp. 3919–3921.
4. D. R. Tanner and A. F. Peterson, "Vector Expansion Functions for the Numerical Solution of Maxwell's Equations," *Microwave Opt. Technol. Lett.*, Vol. 2, Sept. 1989, pp. 331–334.
5. A. R. Pinchuk, C. W. Crowley, and P. P. Silvester, "Spurious Solutions to Vector Diffusion and Wave Field Problems," *IEEE Trans. Magn.*, Vol. 24, Jan. 1988, pp. 158–161.
6. W. R. Scott, "Errors Due to Spatial Discretization and Numerical Precision in the Finite-Element Method," *IEEE Trans. Antennas Propagat.*, Vol. 42, Nov. 1994, pp. 1565–1570.

7. R. Mullen and T. Belytschko, "Dispersion Analysis of Finite Element Semidiscretizations of the Two-Dimensional Wave Equation," *Int. J. Numer. Methods Eng.*, Vol. 18, 1982, pp. 11–29.
8. D. R. Lynch, K. D. Paulsen, and J. W. Strohbehn, "Finite Element Solution of Maxwell's Equations for Hyperthermia Treatment Planning," *J. Comput. Phys.*, Vol. 58, 1985, pp. 246–269.
9. R. Lee and A. Cangellaris, "A Study of Discretization Error in the Finite Element Approximation of Wave Solutions," *IEEE Trans. Antennas Propagat.*, Vol. 40, May 1992, pp. 542–548.
10. G. S. Warren and W. R. Scott, "An Investigation of Numerical Dispersion in the Vector Finite Element Method Using Quadrilateral Elements," *IEEE Trans. Antennas Propagat.*, Vol. 42, Nov. 1994, pp. 1502–1508.
11. J. Jin, *The Finite Element Method in Electromagnetics*, 1st Ed., John Wiley & Sons, New York, 1993.
12. P. P. Silvester and R. L. Ferrari, *Finite Elements for Electrical Engineers*, 2nd Ed., Cambridge University Press, Cambridge, 1990.
13. A. Chaterjee, J. M. Jin, and J. L. Volakis, "Computation of Cavity Resonances Using Edge-Based Finite Elements," *IEEE Trans. Microwave Theory Tech.*, Vol. 40, Nov. 1992, pp. 2106–2108.

CCC 0895-2477/98

developed [1–14], some of which can also be applied to the reconstruction of impenetrable PEC objects. In this case, asymptotic techniques—such as the diffraction tomography approach [15, 16] based on physical optics principles—can be used.

Otherwise, some methods, based on equivalent source principles, have been recently developed for acoustic inverse-scattering problems [17]. A similar electromagnetic problem has been addressed in [18] by using multifilament current sources, while in [19], equivalent currents are placed inside the unknown object, and the problem inversion is done by a curve fitting of the reconstructed contour.

In this letter, we propose a new method based on the application of the *generalized multipole technique* (GMT) [20] to electromagnetic two-dimensional (2-D) TM inverse-scattering problems. A set of multipolar sources is placed within a closed surface which is known to be included in the PEC scatter. The multipolar coefficients of the sources are calculated from measured data that have been previously obtained at a set of observation points. Once the multipolar coefficients are estimated, the shape of the object is straight-